

Supporting Information

Controlled Radical Polymerization and In-Depth Mass-Spectrometric Characterization of Poly(Ionic Liquids) and their Photopatterning on Surfaces

Jan Steinkoenig,^{a,b} Fabian R. Bloesser,^{a,b} Birgit Huber,^c Alexander Welle,^{a,b} Vanessa Trouillet,^d Steffen M. Weidner,^e Leonie Barner,^c Peter W. Roesky,^f Jiayin Yuan,^{*g} Anja S. Goldmann,^{*a,b} and Christopher Barner-Kowollik^{*a,b,c}

^aPreparative Macromolecular Chemistry, Institut für Technische Chemie und Polymerchemie, Karlsruhe Institute of Technology (KIT), Engesserstr. 18, 76128 Karlsruhe, Germany

^bInstitut für Biologische Grenzflächen, Karlsruhe Institute of Technology (KIT), Hermann-von-Helmholtz-Platz 1, 76344 Eggenstein-Leopoldshafen, Germany. E-mail: christopher.barner-kowollik@kit.edu; anja.goldmann@kit.edu

^cSoft Matter Synthesis Laboratory, Institut für Biologische Grenzflächen, Karlsruhe Institute of Technology (KIT), Hermann-von-Helmholtz-Platz 1, 76344 Eggenstein-Leopoldshafen, Germany

^dInstitute for Applied Materials (IAM-ESS) and Karlsruhe Nano Micro Facility (KNMF), Karlsruhe Institute of Technology (KIT), 76344 Eggenstein-Leopoldshafen, Germany

^eBAM-Federal Institute for Materials Research and Testing, Richard-Willstätter-Straße 11, 12489 Berlin, Germany

^fInstitut für Anorganische Chemie, Karlsruhe Institute of Technology (KIT), 76128 Karlsruhe, Germany

^gMax-Planck-Institute of Colloids and Interfaces, Research Campus Golm, 14424 Potsdam, Germany. E-mail: Jiayin.Yuan@mpikg.mpg.de

Materials

All solvents were obtained from Sigma-Aldrich, Acros Organics or Fischer and used without further purification. Absolute solvents were purchased from Acros Organics and stored under nitrogen and over molecular sieves. Triethylamine was refluxed over CaH_2 , freshly distilled under inert atmosphere and stored over molecular sieves (3 Å) at 4 °C. All other reactants were used without further purification. The dialysis tubes were purchased from Spectra/Por (Spectra/Por 7 Dialysis RC Tubing). 1-(chloromethyl)-4-vinylbenzene (90%, Sigma-Aldrich), 2-cyano-2-propyl dodecyl trithiocarbonate (97%, Sigma-Aldrich), 1,2-dimethylimidazole (98%, Acros), 1,1'-azobiscyclohexanecarbonitrile (VAZO-88) (98%, Sigma-Aldrich), 1-butylimidazole (98%, Sigma-Aldrich), LiTf_2N (99%, Acros), $\text{CuSO}_4 \cdot 5 \text{H}_2\text{O}$ (99%, Acros), $\text{K}_2\text{S}_2\text{O}_8$ (97%, abcr), 2,3-dimethylanisole (97%, abcr), AlCl_3 (99%, Acros), methyl-4-bromomethyl benzoate (97%, Fischer), potassium carbonate (99%, Roth), NaOH (99%, Roth), 18-crown-6 (98%, TCI), 4-(dimethylamino)pyridine (99% Sigma-Aldrich), N-(3-dimethylaminopropyl)-N'-ethylcarbodiimide hydrochloride (99%, Sigma-Aldrich), thionyl chloride (>99%, Sigma-Aldrich), (3-aminopropyl)triethoxysilane (99%, Sigma-Aldrich), 4-maleimidobutyric acid (98%, TCI), H_2O_2 (35%, Roth), sulphuric acid (96%, Roth), hydrochloric acid (37%, Roth), sodium hydrogencarbonate (99%, Roth).

Characterization Methods

Size exclusion chromatography (SEC). THF SEC was performed on an Agilent Series 1200 HPLC system, comprising an autosampler, one SDV column (particle size 10 μm , dimension 300 \times 8 mm, porosity 1000 Å) and a UV/vis detector using THF/10 mM LiTf_2N /10 mM *n*-butylimidazole as the eluent at 35 °C with a flow rate of 1 $\text{mL}\cdot\text{min}^{-1}$. The SEC system was calibrated using linear polystyrene standards ranging from 470 to 2.5⁶ $\text{g}\cdot\text{mol}^{-1}$. Appropriate SEC calibrations were carried out relative to a polystyrene calibration (Mark Houwink parameters $K = 14.1 \cdot 10^{-5} \text{ dL}\cdot\text{g}^{-1}$; $\alpha = 0.7$).

Water-based SEC was performed on a PSS WinGPC, comprising an autosampler, a PSS Novema Max precolumn, one PSS Novema Max (particle size 10 μm , dimension 8.00 \times 300.00 mm, porosity 30 Å), two PSS Novema Max (particle size 10 μm , dimension 8.00 \times 300.00 mm, porosity 1000 Å), and a differential refractive index detector (PSS SECcurity RI) as well as an UV detector (PSS SECcurity UV) using water, 0.5 $\text{g}\cdot\text{L}^{-1}$ NaCl and 0.3 M formic acid as the eluent at 30 °C with a flow rate of 1 $\text{mL}\cdot\text{min}^{-1}$. The SEC system was calibrated using linear poly(2-vinyl pyridine) standards ranging from 1100 to 1.06 \cdot 10⁶ $\text{g}\cdot\text{mol}^{-1}$. SEC calibration was carried out relative to poly(2-vinyl pyridine) calibrations (Mark Houwink parameters $K = 2.5 \cdot 10^{-5} \text{ dL}\cdot\text{g}^{-1}$; $\alpha = 0.93$)¹.

¹ American Polymer Standard Corporation (<http://www.ampolymer.com/Mark-HouwinkParameters.html>)

Electrospray ionization mass spectrometry (ESI-MS). Spectra were recorded on a LXQ mass spectrometer (Thermo Fisher Scientific) equipped with an atmospheric pressure ionization source operating in the nebulizer assisted electrospray mode. The instrument was calibrated in the m/z range 192 – 1822 using a standard containing caffeine, Met-Arg-Phe-Ala acetate (MRFA) and a mixture of fluorinated phosphazenes (Ultramark 1621) (all from Sigma-Aldrich). A constant spray voltage 6 kV was used and nitrogen at a dimensionless sweep gas flow rate of 2 (approximately 3 L·min⁻¹) and a dimensionless sheath gas flow rate of 5 (approximately 0.5 L·min⁻¹) were applied. The capillary voltage, the tube lens offset voltage and the capillary temperature were set to 10 V, 70 V, and 300 °C, respectively. The samples were dissolved in the appropriate solvent (see table of assignments Table S2, S3 and S4) in a concentration of 0.1 g·L⁻¹ and infused with a flow rate of 10 µL·min⁻¹.

Matrix assisted laser desorption ionization – time of flight mass spectrometry (MALDI-ToF MS). Spectra were recorded on a Bruker Autoflex III with an acceleration voltage of 20 kV and a neodymium-doped yttrium aluminium garnet (Nd:YAG) (tripled) 355 nm laser. The matrix material consisted of trans-2-[3-(4-*tert*-butylphenyl)-2-methyl-2-propenylidene]malonitrile (DCTB) dissolved in THF with a concentration of 20 g·L⁻¹ and the samples dissolved in methanol with a concentration of 4 g·L⁻¹ and crystallized in a ratio of 10:1 (matrix:sample). The time of flight mode was set to linear mode.

Nuclear magnetic resonance (NMR) spectroscopy. Proton nuclear magnetic resonance (¹H NMR) spectra were recorded on a Bruker AM 400 (400 MHz) spectrometer. Chemical shifts are expressed in parts per million (ppm) and calibrated on characteristic solvent signals as internal standards. All coupling constants are absolute values and J values are expressed in Hertz (Hz). The description of signals include: s = singlet, bs = broad singlet, d = doublet, dd = double doublet, t = triplet, q = quartet, m = multiplet.

Carbon nuclear magnetic resonance (¹³C NMR) spectra were recorded on a Bruker AM 400 (100 MHz) spectrometer.

X-Ray photoelectron spectroscopy (XPS). XPS measurements were performed using a K-Alpha + XPS spectrometer (Thermo Fisher Scientific, East Grinstead, UK). Data acquisition and processing using the Thermo Avantage software is described elsewhere.² All thin films were analyzed using a microfocused, monochromated Al K α X-ray source (400 µm spot size). The K-Alpha charge compensation system was employed during analysis, using electrons of 8 eV energy, and low-energy argon ions to prevent any localized charge build-up. The kinetic energy of the electrons was measured by a 180° hemispherical energy analyzer operated in the constant analyzer energy mode (CAE) at 50 eV pass energy for

² K. L. Parry, A. G. Shard, R. D. Short, R. G. White, J. D. Whittle, A. Wright, *Surf. Interface Anal.*, **2006**, *38*, 1497.

elemental spectra. The spectra were fitted with one or more Voigt profiles (BE uncertainty: ± 0.2 eV) and Scofield sensitivity factors were applied for quantification.³ All spectra were referenced to the C1s peak (C-C, C-H) at 285.0 eV binding energy controlled by means of the well known photoelectron peaks of metallic Cu, Ag, and Au, respectively.

Time-of-flight secondary ion mass spectrometry (ToF-SIMS). ToF-SIMS was performed on a TOF.SIMS5 instrument (ION-TOF GmbH, Münster, Germany), equipped with a Bi cluster primary ion source and a reflectron type time-of-flight analyzer. UHV base pressure was $< 5 \times 10^{-9}$ mbar. For high mass resolution the Bi source was operated in the “high current bunched” mode providing short Bi_3^+ primary ion pulses at 25 keV energy and a lateral resolution of approx. 4 μm . The short pulse length of 1.1 ns allowed for high mass resolution. Primary ion doses were kept below 10^{11} ions/ cm^2 (static SIMS limit). Spectra were calibrated on the omnipresent C^+ , C_2^+ , C_3^+ , or on the C^+ , CH^+ , CH_2^+ , and CH_3^+ peaks. Based on these datasets the chemical assignments for characteristic fragments were determined. Images larger than the maximum deflection range of the primary ion gun of $500 \times 500 \mu\text{m}^2$ were obtained using the manipulator stage scan mode.

Optimization of the water-based SEC

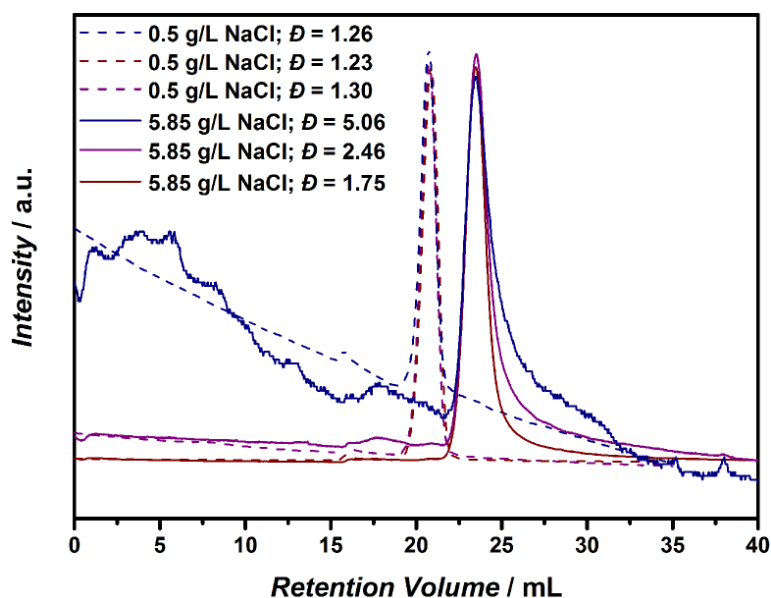


Figure S1: Original SEC traces of p([BVBIM]Cl) (**3**) measured in water/0.3 M formic acid as the eluent at 30 °C. A concentration series with concentrations of 0.5 $\text{g}\cdot\text{L}^{-1}$ (**blue**), 1.0 $\text{g}\cdot\text{L}^{-1}$ (**purple**), and 2.0 $\text{g}\cdot\text{L}^{-1}$ (**brown**) was investigated with two concentrations of NaCl: 5.85 $\text{g}\cdot\text{L}^{-1}$ (0.1 M) (**solid line**), and 0.5 $\text{g}\cdot\text{L}^{-1}$ (**dashed line**).

³ J. H. Scofield, *J. Electron Spectr. Relat. Phen.*, **1976**, 8, 129.

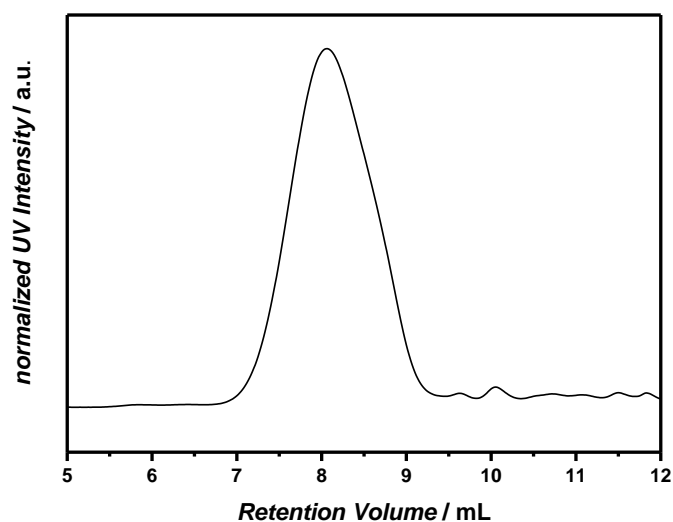


Figure S2: SEC trace of p([BVBIM]Tf₂N) (**4**) ($M_n = 7300 \text{ g}\cdot\text{mol}^{-1}$; $D = 1.28$; $DP_n = 30$) after salt metathesis of p([BVBIM]Cl) (**3**) ($M_n = 8900 \text{ g}\cdot\text{mol}^{-1}$; $D = 1.55$; $DP_n = 37$) measured in a THF solution containing 10 mM LiTf₂N and 10 mM *n*-butylimidazole as the eluent at 35 °C.

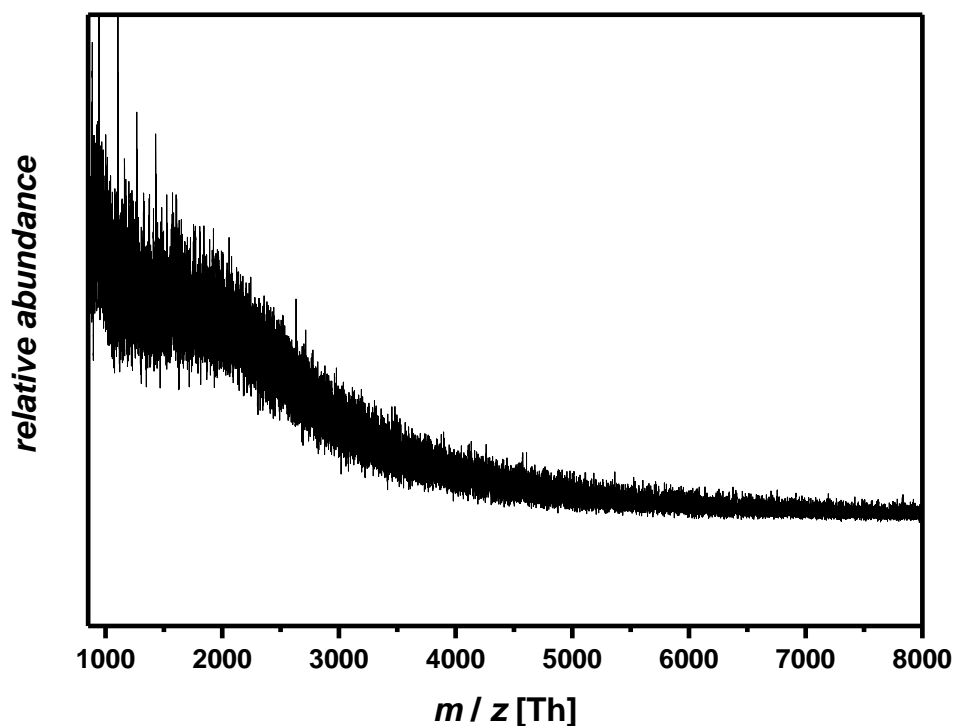


Figure S3: MALDI spectrum of p([BVBIM]Cl) (**3-1**) with DHB as matrix and methanol as solvent in a ratio of 10:1 recorded from $m/z = 1000 \text{ Th}$ to $m/z = 8000 \text{ Th}$. As expected, no polymer pattern is seen with DHB as acidic matrix.

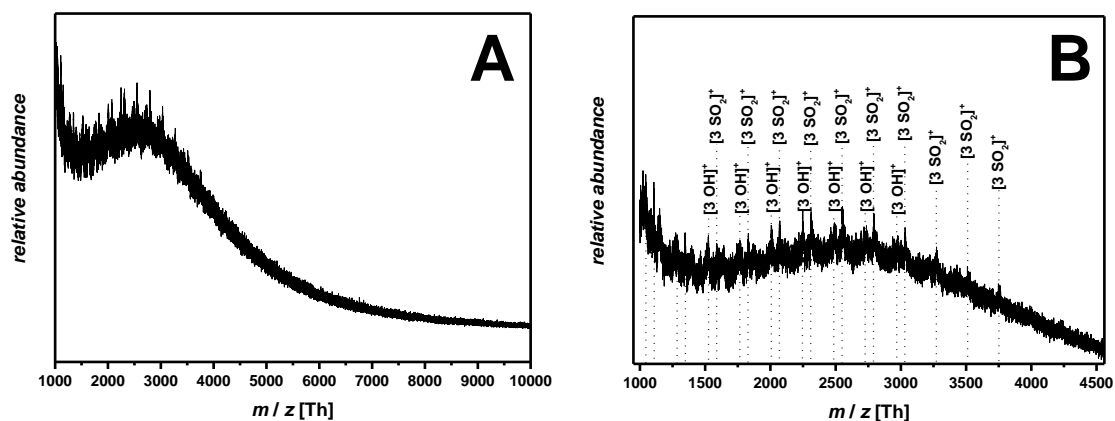


Figure S4: MALDI spectrum of p([BVBIM]Cl) (**3**) recorded after 3 d storage in THF for endgroup conversion. For the MALDI-ToF measurement, methanol was employed as solvent and DCTB as matrix: **(A)** overview spectrum; **(B)** zoom into the spectrum from $m/z = 1000$ Th to $m/z = 4500$ Th. For the structure of $[3 \text{ OH}]$ and $[3 \text{ SO}_2]$ refer to Fig. 5.

Polymerization in different solvents

Table S1 RAFT polymerization of [BVBIM]Cl (**1**) employing ethanol and DMSO/water (1:1, v/v) as solvents.

Entry	<i>Ethanol</i>						<i>H₂O/DMSO (1:1, v/v)</i>					
	<i>t</i>	$M_n^{\text{theo.}}$	M_n^{NMR}	M_n^{SEC}	\bar{D}^{SEC}	<i>Conv.</i>	<i>t</i>	$M_n^{\text{theo.}}$	M_n^{NMR}	M_n^{SEC}	\bar{D}^{SEC}	<i>Conv.</i>
	[h]	[g mol ⁻¹]	[g mol ⁻¹]	[g mol ⁻¹]			[h]	[g mol ⁻¹]	[g mol ⁻¹]	[g mol ⁻¹]		
1	2	5100	6200	1100	6.44	13	2	5000	3700	2300	2.0	20
2	4	8900	8700	11700	1.90	23	4	6300	4000	4000	1.7	25
3	5	13300	12000	17000	1.69	35	6	12000	8000	8200	1.6	48
4	8	17400	15000	20000	1.76	47	8	16000	6400	8900	1.6	67

NMR spectra of the monomers 1, 2 and 5 and of the polymers 3 and 4

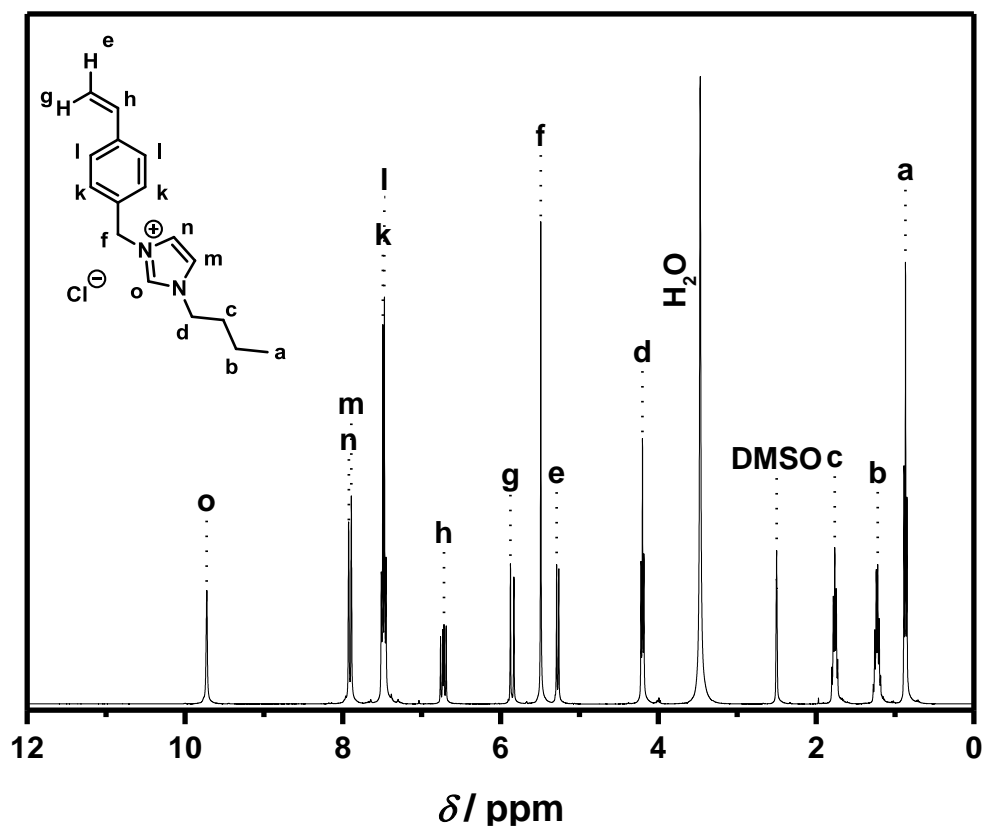


Figure S5: ^1H NMR of monomer 1 in DMSO at 400 MHz.

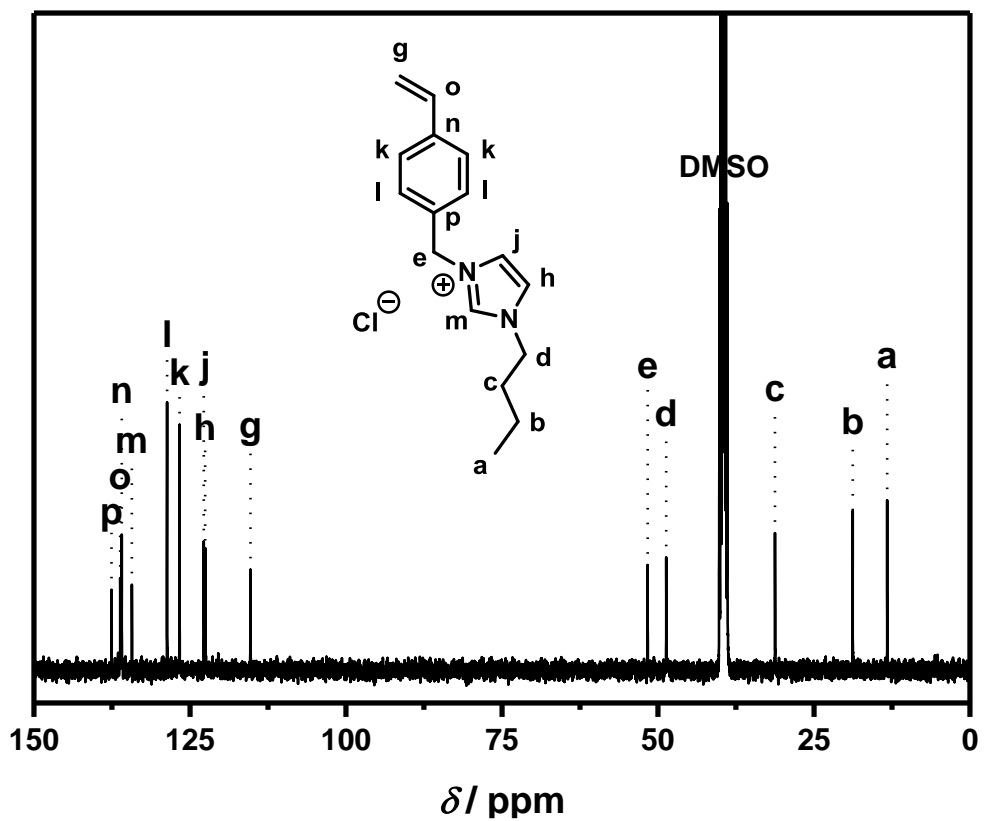


Figure S6: ^{13}C NMR of monomer 1 in DMSO at 100 MHz.

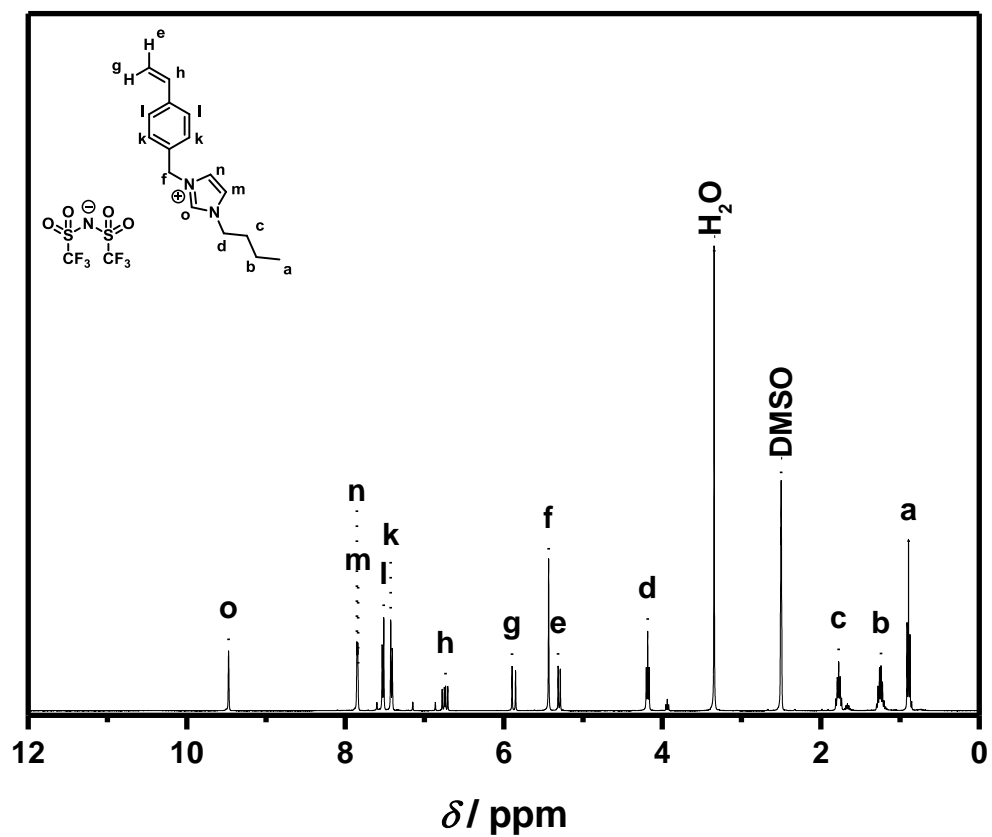


Figure S7: ^1H NMR of monomer **2** in DMSO at 400 MHz.

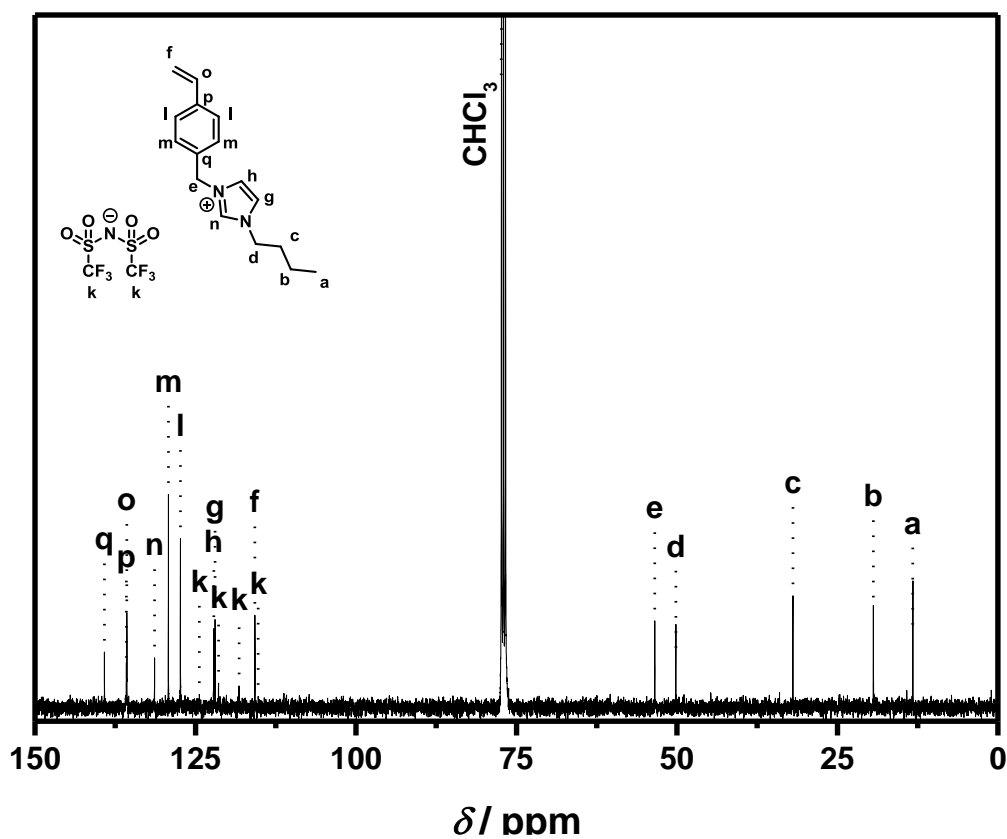


Figure S8: ^{13}C NMR of monomer **2** in DMSO at 100 MHz.

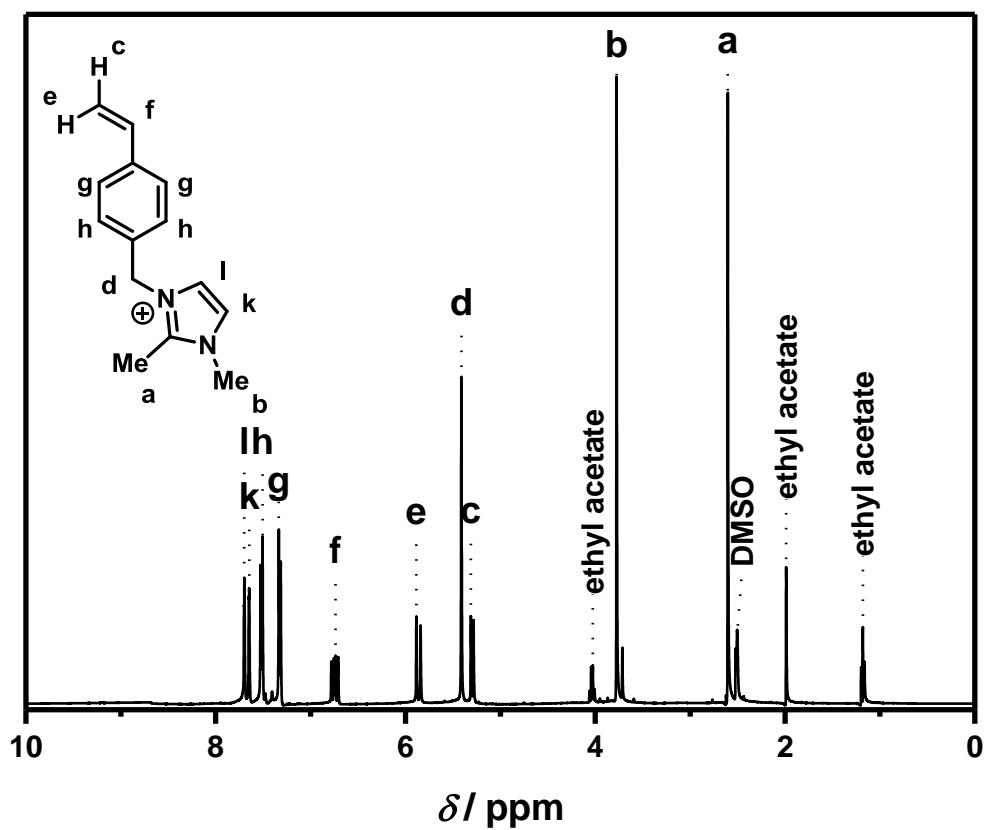


Figure S9: ^1H NMR of monomer **5** in DMSO at 400 MHz.

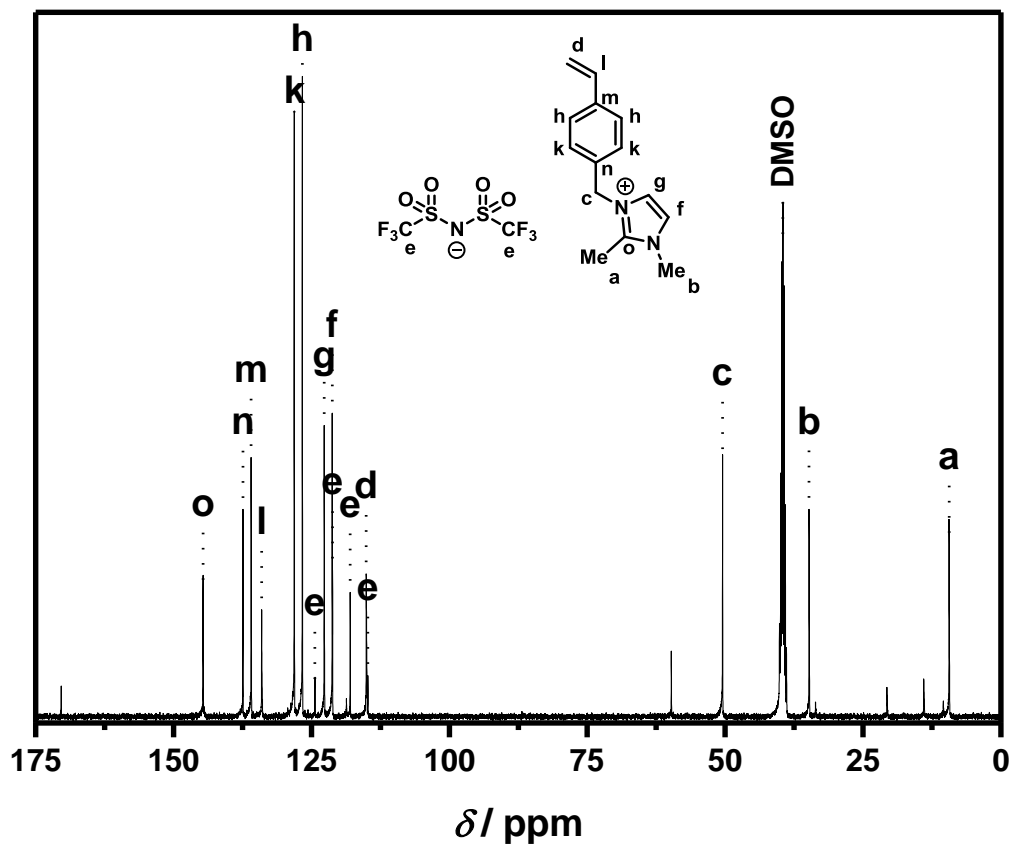


Figure S10: ^{13}C NMR of monomer **5** in DMSO at 100 MHz.

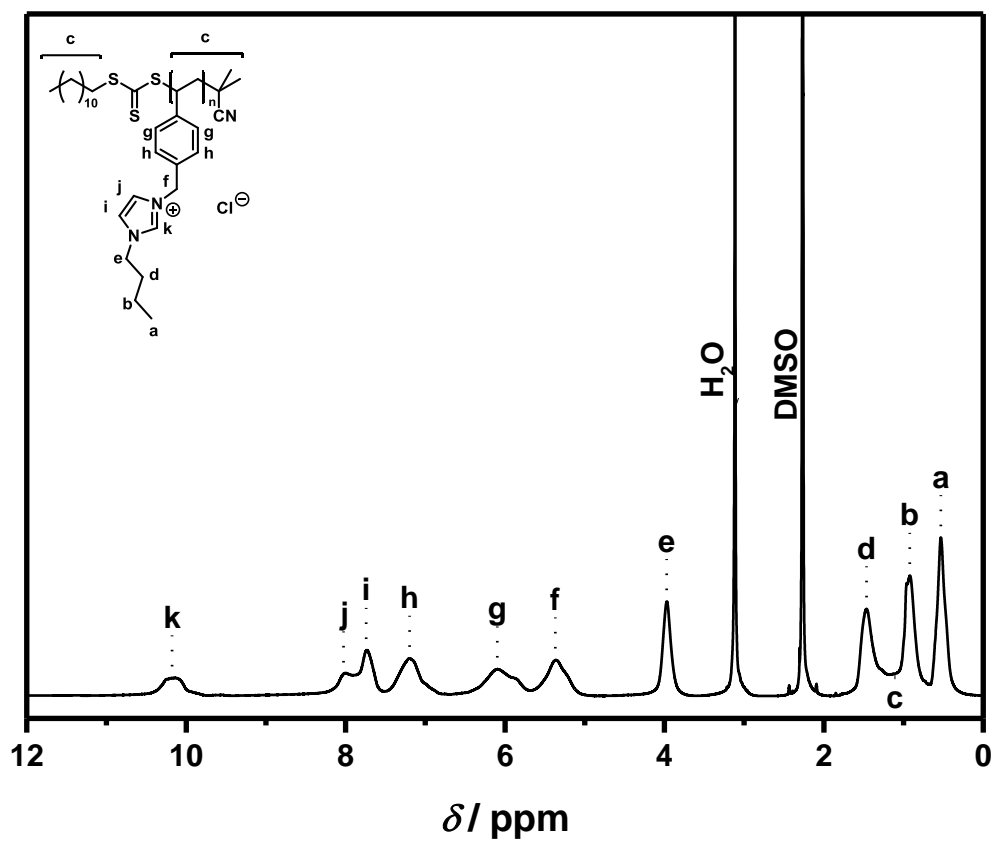


Figure S11: ^1H NMR of polymer **3** in DMSO at 400 MHz.

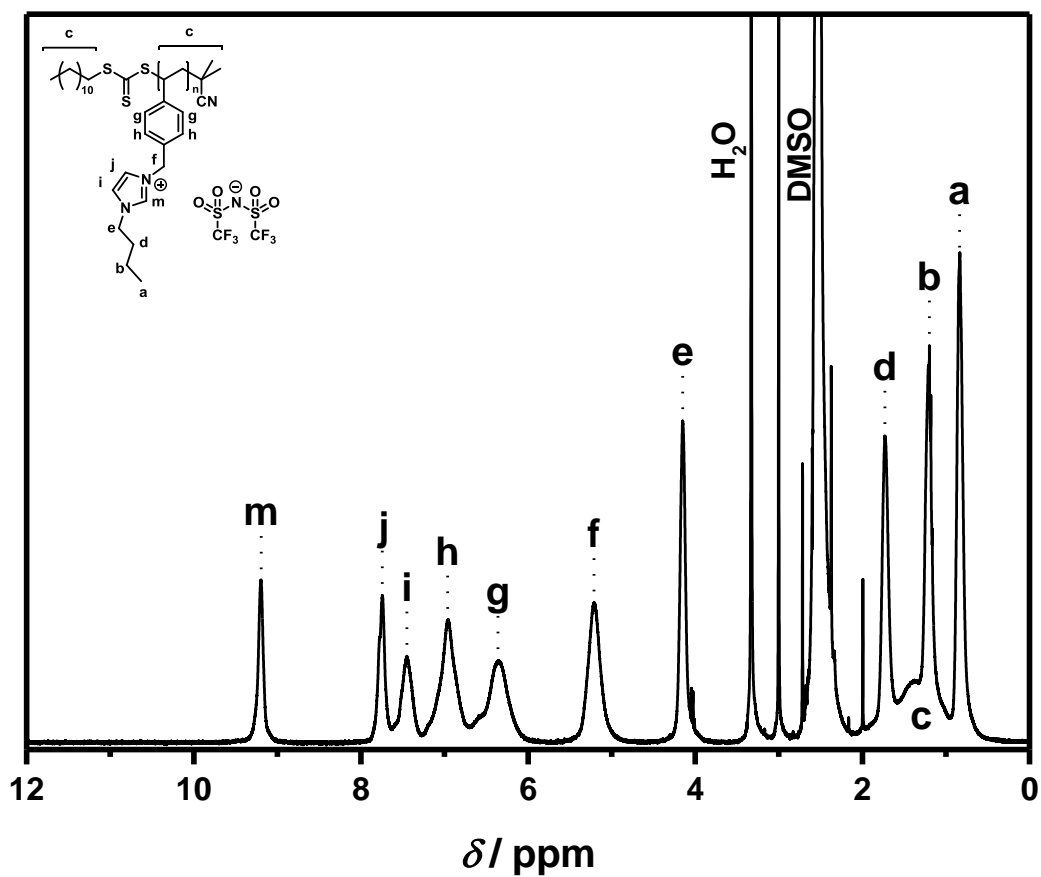


Figure S12: ^1H NMR of polymer **4** in DMSO at 400 MHz.

List of assignments

Table S2: Peak assignments of the MALDI spectrum of p([BVBIM]Cl) (**3-1**) from $m/z = 1000$ Th to $m/z = 12000$ Th.

Label	m/z (theo) [Th]	m/z (exp) [Th]	$\Delta m/z$ [Th]
[3 _{b,d}] ⁺	1026.48	1026.63	0.15
[3 _b] ⁺	1066.65	1066.73	0.08
[3 _{a,b}] ⁺	1102.62	1102.72	0.10
[3 _{a,b}] ⁺	1138.59	1138.64	0.05
[3 _{a,d}] ⁺	1180.51	1180.81	0.30

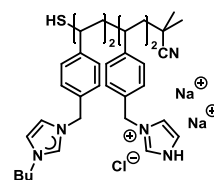
Table S3: Peak assignments of the MALDI spectrum of p([BVBIM]Tf₂N) (**4**) from $m/z = 2000$ Th to $m/z = 2400$ Th.

Label	m/z (theo) [Th]	m/z (exp) [Th]	$\Delta m/z$ [Th]
[4 '] ⁺	2079.28	2079.38	0.10
[4 _{a,b}] ⁺	2149.59	2149.32	0.26
[4 '] ⁺	2263.50	2263.65	0.15
[4 _{a,d}] ⁺	2396.43	2396.29	0.14

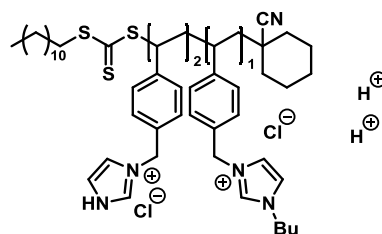
Table S4: Peak assignments of the ESI-MS spectrum of p([BVBIM]Cl) (**3**) ($M_w = 1900 \text{ g}\cdot\text{mol}^{-1}$) from $m/z = 200 \text{ Th}$ to $m/z = 900 \text{ Th}$ (THF/MeOH (3:2, v/v)).

Label	m/z (theo) [Th]	m/z (exp) [Th]	$\Delta m/z$ [Th]	Structure
[M] ⁺	241.17	241.20	0.03	
[3 _{b,c'}] ²⁺	274.64	274.76	0.12	
[3 _{b,c'} '] ³⁺	343.54	343.60	0.06	
[3 _b] ³⁺	356.22	356.24	0.02	
[3 _{c,d*}] ³⁺	394.72	394.76	0.04	
[3 _b] ²⁺	413.75	413.80	0.05	
[3 _{c*}] ²⁺	480.74	480.84	0.10	
[3 _{b,d}] ²⁺	513.74	513.84	0.10	

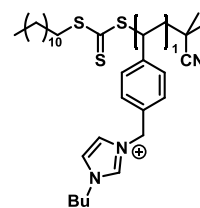
[3c']²⁺ 533.73 533.72 0.01



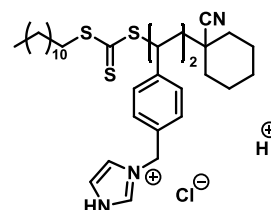
[3a,c]³⁺ 551.75 551.72 0.03



[3b]⁺ 586.32 586.36 0.04



[3d*]⁺ 826.35 826.28 0.07



[3a,b]⁺ 862.46 862.40 0.06

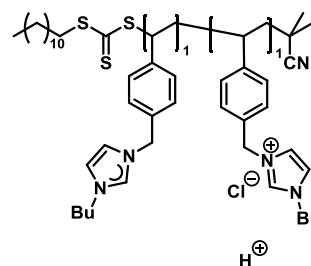


Table S5: Peak assignments of the ESI-MS spectrum of p([BVBIM]Tf₂N) (**4**) from m/z = 400 Th to m/z = 1200 Th (acetonitrile/water (1:1, v/v)).

Label	m/z (theo)	m/z (exp)	$\Delta m/z$	Structure
[4 _b] ²⁺	413.75	413.74	0.01	
[4 _b] ⁺	586.32	586.33	0.01	
[4 _{a,b}] ²⁺	674.29	674.36	0.07	
[4 _d] ³⁺	760.95	760.90	0.05	
[4 _{a,c}] ³⁺	849.25	849.09	0.16	
[4 _{a,b}] ³⁺	878.37	878.09	0.28	
[4 _{a,d}] ²⁺	934.84	935.00	0.16	

$[4_{a,b}]^{3+}$	1052.07	1052.09	0.02	
$[4_{a,b}]^+$	1107.42	1107.55	0.13	

Miscellaneous XP Spectra

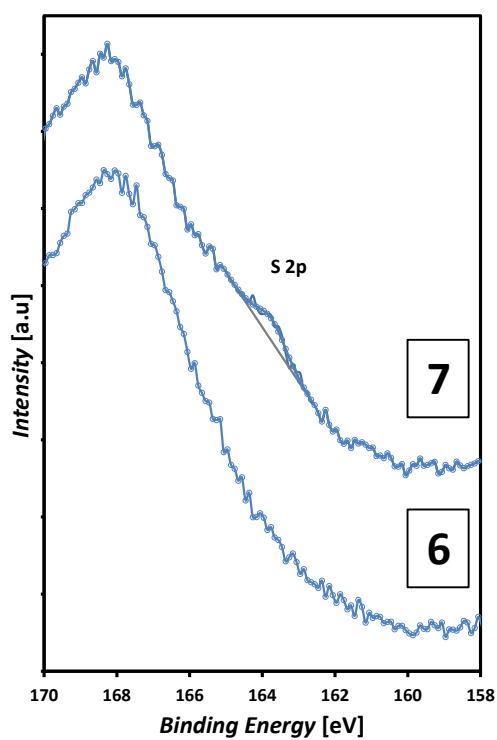


Figure S13: S 2p XP spectra of the maleimide-coated surface (**6**) in comparison to the RAFT-functionalized surface (**7**). In the case of surface (**7**), the sulphur doublet (163.6 eV) appears in the range of the broad plasmon peak of the silicon.

Photoreactor

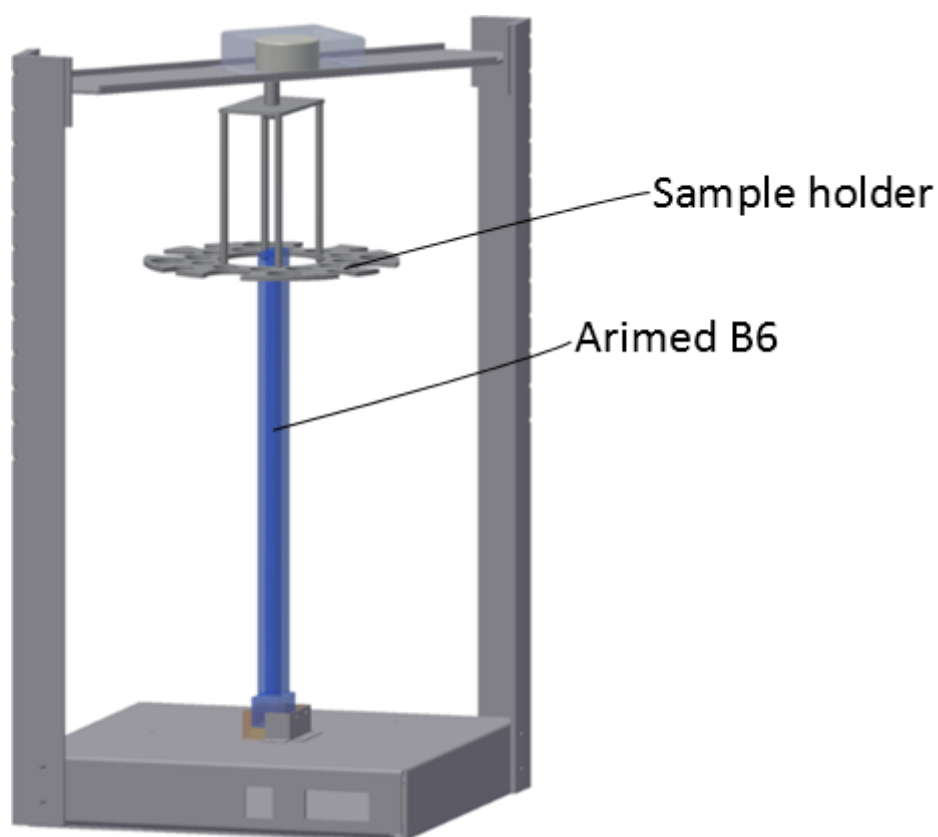


Figure S14: Schematic representation of the custom-built photoreactor employed in the current study for the surface-patterning of PILs with the Arimed B6 bulb in the middle with a motor operated carousel as sample holder.

Sample holders and photomasks

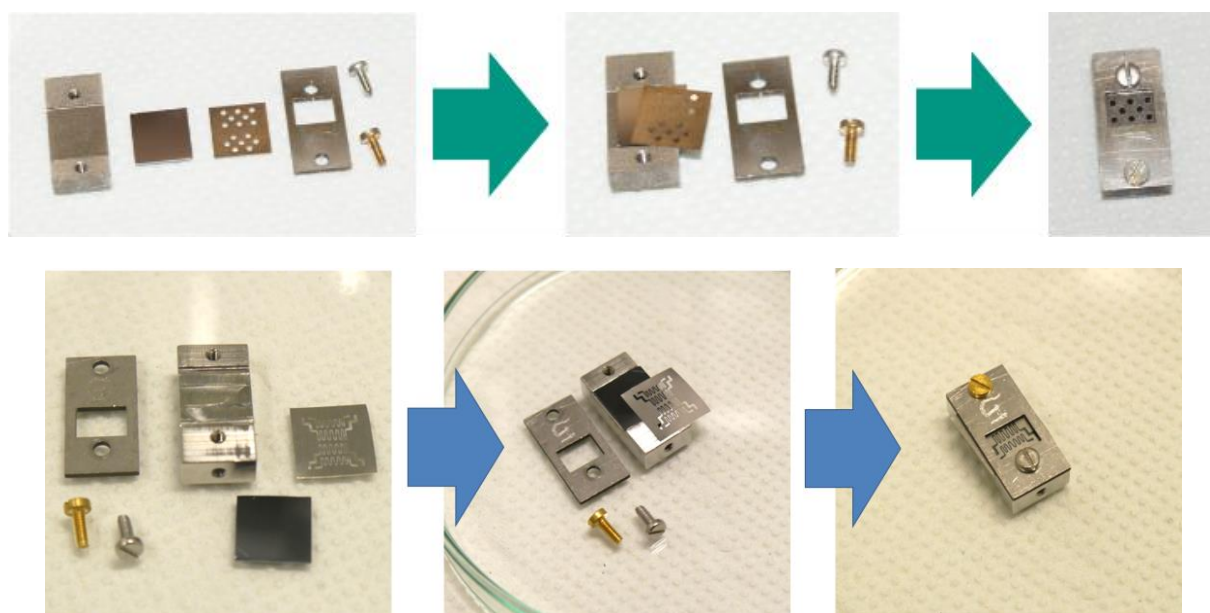


Figure S15: Sample holders and the shadow masks utilized for the reaction to obtain the dotted pattern (top) and the meander structure (below) on the surfaces.

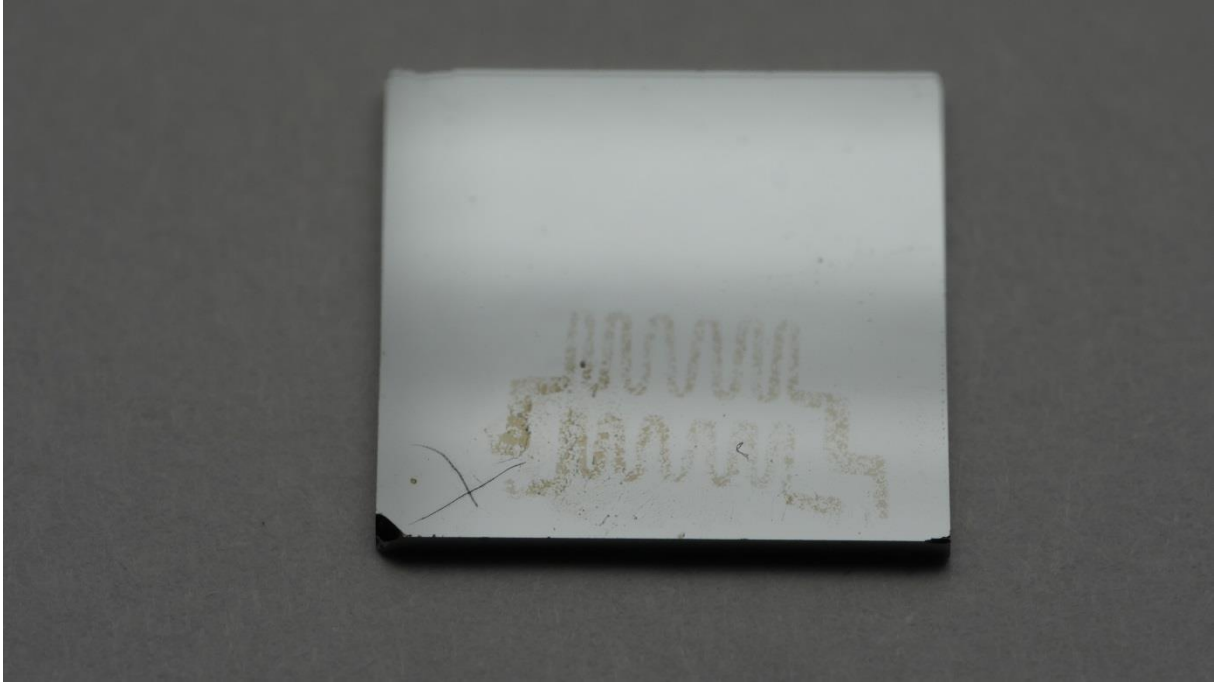


Figure S16: Photograph taken from surface 9 with the meander shaped structure.